August, 2004

Above-Room-Temperature Ferromagnetic Ni2+:ZnO Thin Films Prepared from Colloidal Diluted Magnetic Semiconductor Quantum Dots

D. A. Schwartz
Kevin R. Kittilstved, *University of Massachusetts - Amherst*
D. R. Gamelin

AIP | Applied Physics Letters

Above-room-temperature ferromagnetic Ni2+-doped ZnO thin films prepared from colloidal diluted magnetic semiconductor quantum dots

Dana A. Schwartz, Kevin R. Kittilstved, and Daniel R. Gamelin

Citation: Appl. Phys. Lett. **85**, 1395 (2004); doi: 10.1063/1.1785872
View online: http://dx.doi.org/10.1063/1.1785872
View Table of Contents: http://apl.aip.org/resource/1/APPLAB/v85/i8
Published by the American Institute of Physics.

Above-room-temperature ferromagnetic Ni^{2+}-doped ZnO thin films prepared from colloidal diluted magnetic semiconductor quantum dots

Dana A. Schwartz, Kevin R. Kittilstved, and Daniel R. Gamelin[a)]
Department of Chemistry, Box 351700, University of Washington, Seattle, Washington 98195-1700

(Received 4 November 2003; accepted 25 June 2004)

We report the preparation of spin-coated nickel-doped zinc oxide nanocrystalline thin films using high-quality colloidal diluted magnetic semiconductor (DMS) quantum dots as solution precursors. These films show robust ferromagnetism with Curie temperatures above 350 K and 300 K saturation moments up to 0.1 Bohr magnetons per nickel. These results demonstrate a step toward the use of colloidal zero-dimensional DMS nanocrystals as building blocks for the bottom-up construction of more complex ferromagnetic semiconductor nanostructures. © *2004 American Institute of Physics*. [DOI: 10.1063/1.1785872]

Diluted magnetic semiconductors (DMSs)[1] are currently receiving intense theoretical and experimental attention because of the central role they may play in the emerging field of spintronics.[2] Functional spintronic devices, such as spin light-emitting diodes, have been demonstrated using II–VI and III–V DMSs as the pivotal spin-injection components, but to date these devices have been operable only at cryogenic temperatures because of either the absence of ferromagnetism or the low Curie temperature (T_C) for the ferromagnetic phase transition.[3] The development of practical semiconductor spintronics devices will thus require the development of new DMSs with Curie temperatures well above room temperature. Computational studies have predicted ferromagnetism above room temperature for several ZnO-based DMSs.[4] Some of these predictions have recently been verified experimentally by the observation of high-T_C ferromagnetism in thin films of Co^{2+}-, Fe^{2+}-, Mn^{2+}-, and V^{2+}-doped ZnO.[5–8]

Nanoscale DMSs are key components of many potential spintronics devices.[2,9] The properties of this class of materials, and particularly oxide DMS nanocrystals, remain largely unexplored, however. We have initiated a systematic study of nanocrystalline oxide DMSs synthesized by solution chemical routes, and have recently reported direct chemical methods for the synthesis and purification of high-quality internally doped colloidal ZnO DMS quantum dots (QDs).[8,10,11] These solution synthetic methods allow the speciation of magnetic dopant ions to be controlled chemically, and thereby provide an avenue for avoiding the formation of undesired magnetic phases. In this letter, we report the use of colloidal Ni^{2+}-doped ZnO (Ni^{2+}:ZnO) DMS nanocrystals as solution precursors for the preparation of nanostructured ZnO thin films. These films show robust ferromagnetism with Curie temperatures above 350 K. These results illustrate a bottom-up approach for the assembly of ferromagnetic semiconductor nanostructures. This approach suggests many opportunities for the application of DMS nanocrystals in nanotechnology.

1.5% Ni^{2+}:ZnO nanocrystals capped with trioctylphosphine oxide (TOPO) and resuspended in toluene were prepared and characterized as reported previously.[10] Ni^{2+} concentrations were quantified by inductively coupled plasma atomic emission spectrometry. Figure 1(a) shows a representative transmission electron microscopy (TEM) image of TOPO-capped Ni^{2+}:ZnO DMS-QDs deposited on a lacey carbon grid from a clear toluene colloidal suspension. The doping of open-shell impurity ions into the ZnO lattice introduces magnetic properties to this semiconductor, and we have previously shown that the free-standing ZnO DMS-QDs are paramagnetic, not superpara- or ferromagnetic.[10,12] Doping also introduces sub-bandgap optical transitions that can be used to selectively probe the geometric and electronic structures of the dopant ions themselves. Figure 1(b) shows high-resolution low-temperature absorption and magnetic circular dichroism (MCD) spectra of a frozen solution of 1.5% Ni^{2+}:ZnO nanocrystals in the ligand-field energy region. A series of very sharp transitions centered around 15 500 cm^{-1} is observed at cryogenic temperatures that is readily identified as the $^3T_1(F) \rightarrow {}^3T_1(P)$ ligand-field transition of Ni^{2+} ions in the trigonally distorted pseudotetrahedral coordination environment of the cationic site in ZnO. A 30 cm^{-1} trigonal-field splitting of the first electronic origin is

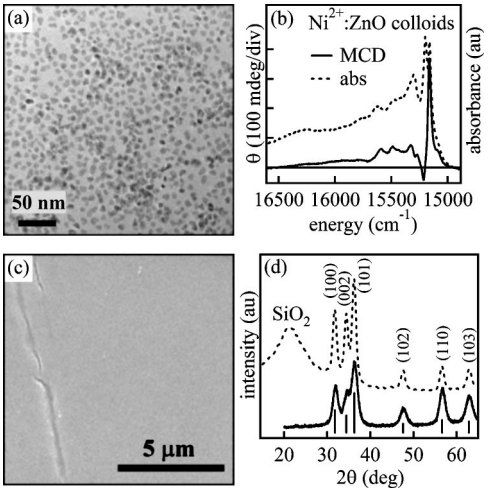

FIG. 1. (a) TEM image of representative TOPO-capped Ni^{2+}:ZnO nanocrystals deposited from colloidal suspension. (b) 7 Tesla, 5 K MCD, and 7 K electronic absorption spectra of a frozen solution of 1.5% Ni^{2+}:ZnO nanocrystals. (c) SEM image of a 1.5% Ni^{2+}:ZnO nanocrystalline thin film prepared by spin coating. (d) XRD of the 1.5% Ni^{2+}:ZnO nanocrystals (solid line) from (b) and the spin-coated Ni^{2+}:ZnO nanocrystalline thin film (dashed line) from (c). The XRD peaks are indexed for wurtzite ZnO.

[a)]Electronic mail: gamelin@chem.washington.edu

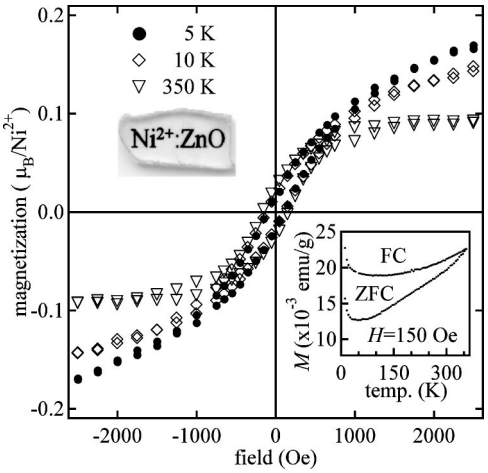

FIG. 2. Magnetization hysteresis loops for the spin-coated 1.5% Ni^{2+}:ZnO nanocrystalline thin film at 5, 10, and 350 K. The data have been corrected only for the diamagnetic background of the substrate, measured at 350 K. The optical transparency of the thin film is demonstrated by the image in the upper left inset. The lower right inset shows ZFC and FC magnetization data collected with an applied field (H) of 150 Oe.

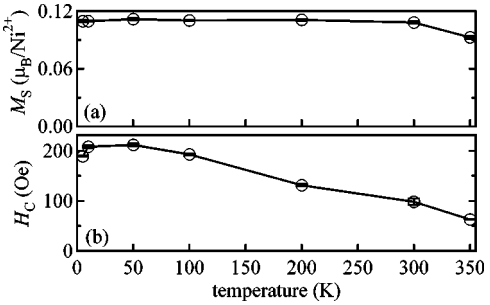

FIG. 3. (a) The ferromagnetic saturation moment (M_S) per nickel and (b) the coercive field (H_C) plotted vs temperature for the spin-coated nanocrystalline thin film from Figs. 1 and 2.

resolved in both the absorption and MCD spectra, as are several vibronic sideband transitions whose energies agree quantitatively with those observed in bulk single-crystal Ni^{2+}:ZnO.[13] The narrow peak widths of the $^3T_1(F) \rightarrow {}^3T_1(P)$ electronic origins (full width at half maximum $\approx 30\ cm^{-1}$) reflect the homogeneity of the Ni^{2+} ions in these nanocrystals.

Nanocrystalline thin films were prepared by spin coating the colloidal Ni^{2+}:ZnO nanocrystals onto fused-silica substrates. The films were heated to 525 °C in air for ~2 min between coats to evaporate the organic solvent and remove surface ligands. Figure 1(c) shows a scanning electron microscopy (SEM) image of the surface of one such nanocrystalline thin film prepared from 20 successive coats of the colloids used for Fig. 1(b). Profilometry measurements show a relatively flat film with a thickness of $2.0 \pm 0.3\ \mu m$ across the entire surface, but some mesoscopic cracks and defects are evident. X-ray diffraction (XRD) data collected for the same film [Fig. 1(d)] show only peaks associated with ZnO. The XRD peaks of the ZnO nanocrystals and the nanocrystalline film are both broadened relative to those of bulk ZnO. Analysis of the diffraction peak widths using the Scherrer equation yields an average particle diameter of ~6.1 nm for the nanocrystals and ~10 nm for the film, consistent with some degree of nanocrystal fusion during the film preparation. We have previously reported that ferromagnetism in aggregates of these and related DMS nanocrystals correlates with the density of aggregation.[10,12] The above spin-coating procedure ensures a densely packed and well interconnected nanocrystalline network that should be conducive to long-range magnetic ordering similar to that observed in the dense aggregates.

The magnetic properties of the thin films were measured using a superconducting quantum interference device magnetometer, and the results for the film from Fig. 1 are presented in Fig. 2. Clear evidence for ferromagnetism above room temperature was observed. At 300 K, a saturation moment of $M_S = 0.11$ Bohr magnetons (μ_B) per Ni^{2+} ($0.019\ emu/cm^3$), a coercive field of $H_C = 100$ Oe, and a remanence of $M_R = 0.11\ \mu_B/Ni^{2+}$ ($M_R = M_S = 10\%$) were observed. This saturation moment is similar to those reported recently for Mn^{2+}:ZnO pellets[7] and Co^{2+}:ZnO (Ref. 10) or Ni^{2+}:ZnO (Ref. 12) nanocrystalline aggregates, but is smaller than some values reported for Co^{2+}:ZnO thin films.[5] The temperature dependence of M_S for the ferromagnetic signal was measured up to 350 K (the instrument limit), and the results are presented in Fig. 3(a). M_S is constant up to 300 K and drops slightly at 350 K. From these data, we conclude that T_C is above 350 K.

The small 300 K coercivity of only 100 Oe and the resulting small hysteresis area are very similar to those of other ferromagnetic ZnO DMSs and nanocrystalline DMS-QD aggregates,[5–7,10,12] and characterize these materials as soft ferromagnets. Although the precise origins of the coercivity in these ZnO DMSs remain uncertain, the majority of the coercivity likely arises from domain-wall pinning effects. Figure 3(b) shows the change in H_C measured over the same temperature range. H_C increases from 185 to 210 Oe upon warming the film from 5 to 50 K and then gradually decreases to 70 Oe when the temperature is raised to 350 K. The gradual decrease in coercivity with increasing temperature is similar to the behavior observed in other ZnO DMSs,[5–7] and is consistent with thermally activated magnetization reversal involving domain-wall pinning. The reduction in H_C below 50 K appears to be atypical, however. We have previously interpreted a similar but more pronounced effect in Ni^{2+}:ZnO aggregates as arising from exchange bias stabilization of ferromagnetic domains by magnetic exchange coupling with surrounding paramagnetic Ni^{2+} ions.[12] The $^3T_1(F)$ ground term of paramagnetic Ni^{2+} in ZnO is subject to large first-order spin–orbit coupling that yields a low-temperature ground state having no first-order Zeeman coefficient (A_1, $J=0$).[14] As a consequence, the effective magnetic moment of paramagnetic Ni^{2+} in ZnO diminishes rapidly as the temperature is lowered below ~100 K, and the energy of the exchange interaction with paramagnetic Ni^{2+} diminishes concomitantly.[12] From the data in Fig. 3(b), this exchange interaction is seen to play a small but significant role in determining the overall coercivity of this film.

In addition to ferromagnetism, substantial superparamagnetism was also evident. Between 5 and 10 K, for example, the 4000 Oe magnetization in Fig. 2 decreases by ~10%. This decrease cannot be attributed to the paramagnetism of Ni^{2+} in ZnO because tetrahedral Ni^{2+} shows only temperature-independent paramagnetism between 5 and 10 K.[14] Instead, we attribute this temperature-dependent magnetization to superparamagnetism that likely arises from magnetic ordering in fused nanocrystalline Ni^{2+}:ZnO do-

mains too small to support ferromagnetism. Further evidence for substantial superparamagnetism comes from the zero-field-cooled (ZFC) and field-cooled (FC) magnetization data shown in Fig. 2, inset. In the ZFC experiment, the magnetization increases with increasing temperature above 20 K, consistent with magnetic ordering. The FC magnetization data also show a slight increase in magnetization as the temperature is raised above 20 K but remain significantly higher than the ZFC data at all temperatures until the instrumental limit is reached. Again, strong temperature dependence is observed below 20 K, where the magnetization of paramagnetic Ni^{2+} in ZnO is temperature independent. These data are consistent with the presence of an ensemble of superparamagnetic domains having a broad range of blocking temperatures in this nanocrystalline thin film, in addition to the presence of stable ferromagnetic domains.

The ferromagnetism of this film could arise from a number of possible sources. Phase segregated NiO nanocrystals are an unlikely source of this ferromagnetism because of the quantitative incorporation of dopants within the ZnO lattice in the DMS-QD precursors and because of the very low Curie temperatures previously observed for NiO nanocrystals (e.g., $T_C < 5$ K).[15] Metallic nickel precipitants are also unlikely candidates because the synthesis and the spin coating of the DMS nanocrystals were both performed under oxidizing conditions in which metallic nickel is unable to form. We therefore conclude that the observed ferromagnetism is an intrinsic property of Ni^{2+}:ZnO. *Ab initio* calculations have been used previously to predict that Ni^{2+}:ZnO will exhibit ferromagnetic ordering in the presence of sufficient *n*-type carriers.[4] In the nanocrystalline thin films reported here, *n*-type dopants have not been deliberately introduced. The observation that free-standing Ni^{2+}:ZnO DMS-QDs are paramagnetic, not superparamagnetic, suggests that the nanocrystals themselves lack the necessary *n*-type character to support magnetic ordering of the dopants. Defects of *n*-type form readily in ZnO,[16] however, and we propose that defects trapped at the interfaces between fused nanocrystals during film preparation provide the necessary *n*-type character to activate long-range magnetic ordering.

Despite the highly disordered nanocrystalline structure of the film used for Figs. 1–3, attempts were made to measure its macroscopic transport properties. The resistivity was found to be beyond our detection limits ($>10^8\ \Omega$ cm). As seen in Fig. 1(c), the film is imperfect on the mesoscale, containing numerous cracks and fissures. The high resistivity is most likely attributable to the presence of these mesoscopic defects, which cause poor electrical contact between adjacent sections of the nanocrystalline ZnO film. Such defects may arise from the large volume occupied by the organic ligands of the colloidal nanocrystals prior to calcination. We estimate that the volume of the material is reduced by ~66% upon calcination, causing contraction and ultimately cracking of the film. Future experiments will address improvement of the conductivity of these films.

In summary, we have demonstrated the preparation of ferromagnetic nanocrystalline thin films of the DMS Ni^{2+}:ZnO by solution processing methods starting from colloidal paramagnetic DMS-QD precursors. These results provide a simple demonstration of the use of colloidal paramagnetic DMS nanocrystals as building blocks to form ferromagnetic semiconductor structures of higher dimensionality. The application of homogeneous DMS nanocrystals as precursors, combined with aerobic processing conditions, largely obviates the formation of undesirable phase-segregated precipitants. This approach offers opportunities for the study of shape, dimensionality, and connectivity effects on room-temperature magnetic ordering in nanoscale DMSs.

Financial support from the NSF (Grant No. ECS-0224138 and DMR-0239325) is gratefully acknowledged. Acknowledgment is also made to the Research Corporation (RI0832) and the Semiconductor Research Corporation (2002-RJ-1051G) for partial support of this research, and to the UW/PNNL Joint Institute for Nanoscience for fellowship support for two of the authors (D.A.S. and K.R.K.). TEM data were collected at the EMSL (PNNL), a user facility sponsored by the DOE and by Battelle. Dr. C. Wang (PNNL), N. Norberg (UW), Dr. P. Blomqvist (UW), and X. Ji (UW) are thanked for valuable experimental assistance. D.R.G. is a Cottrell Scholar of the Research Corporation.

[1] J. K. Furdyna and J. Kossut, in *Semiconductors and Semimetals*, edited by J. K. Furdyna and J. Kossut (Academic, New York, 1988).
[2] S. A. Wolf, D. D. Awschalom, R. A. Buhrman, J. M. Daughton, S. von Molnár, M. L. Roukes, A. Y. Chtchelkanova, and D. M. Treger, Science **294**, 1488 (2001).
[3] Y. Ohno, D. K. Young, B. Beschoten, F. Matsukura, H. Ohno, and D. D. Awschalom, Nature (London) **402**, 790 (1999); B. T. Jonker, Y. D. Park, B. R. Bennett, H. D. Cheong, G. Kioseoglou, and A. Petrou, Phys. Rev. B **62**, 8180 (2000); R. Fiederling, M. Keim, G. Reuscher, W. Ossau, G. Schmidt, A. Waag, and L. W. Molenkamp, Nature (London) **402**, 787 (1999); R. M. Stroud, A. T. Hanbicki, Y. D. Park, G. Kioseoglou, A. G. Petukhov, B. T. Jonker, G. Itskos, and A. Petrou, Phys. Rev. Lett. **89**, 166602 (2002).
[4] K. Sato and H. Katayama-Yoshida, Physica B **308**, 904 (2001).
[5] K. Ueda, H. Tabata, and T. Kawai, Appl. Phys. Lett. **79**, 988 (2001).
[6] Y. M. Cho, W. K. Choo, H. Kim, D. Kim, and Y. Ihm, Appl. Phys. Lett. **80**, 3358 (2002); H. Saeki, H. Tabata, and T. Kawai, Solid State Commun. **120**, 439 (2001).
[7] P. Sharma, A. Gupta, K. V. Rao, F. J. Owens, R. Sharma, R. Ahuja, J. M. O. Guillen, B. Johansson, and G. A. Gehring, Nat. Mater. **2**, 673 (2003).
[8] N. S. Norberg, K. R. Kittilstved, J. E. Amonette, R. K. Kukkadapu, D. A. Schwartz, and D. R. Gamelin, J. Am. Chem. Soc. **126**, 9387 (2004).
[9] D. P. DiVincenzo and D. Loss, J. Magn. Magn. Mater. **200**, 202 (1999).
[10] D. A. Schwartz, N. S. Norberg, Q. P. Nguyen, J. M. Parker, and D. R. Gamelin, J. Am. Chem. Soc. **125**, 13205 (2003).
[11] P. V. Radovanovic, N. S. Norberg, K. E. McNally, and D. R. Gamelin, J. Am. Chem. Soc. **124**, 15192 (2002).
[12] P. V. Radovanovic and D. R. Gamelin, Phys. Rev. Lett. **91**, 157202 (2003).
[13] R. S. Anderson, Phys. Rev. **164**, 398 (1967).
[14] W. N. Brumage and C. C. Lin, Phys. Rev. **134**, 950 (1964).
[15] Y. Ichiyanagi, N. Wakabayashi, J. Yamazaki, S. Yamada, Y. Kimishima, E. Komatsu, and H. Tajima, Physica B **329**, 862 (2003).
[16] D. G. Thomas, Phys. Chem. Solids **3**, 229 (1957).